REVERSIBLE WAVELET AND SPECTRAL TRANSFORMS FOR LOSSLESS COMPRESSION OF COLOR IMAGES

G Uma Rani[1] and Prof G Indumathi[2]

[1]P.G.Scholar, Department of Electronics and Communications, CMRIT, Bangalore
umaranighantasala@gmail.com
[2]Professor, Department of Electronics and Communications, CMRIT, Bangalore
indu_cmrit@rediffmail.com

ABSTRACT

Recent years have seen tremendous increase in the generation, transmission, and storage of color images. A new lossless image compression method for progressive-resolution transmission of color images is carried out in this paper based on spatial and spectral transforms. Reversible wavelet transforms are performed across red, green, and blue color sub bands first. Then adaptive spectral transforms like inter band prediction method is applied on associated color sub bands for image compression. The combination of inverse spectral transform (ST^{-1}) and inverse reversible wavelet transforms (RWT^{-1}) finally reconstructs the original RGB color channels exactly. Simulation of the implemented method is carried out using MATLAB 6.5.

KEYWORDS

Spatial transforms, Spectral decorrelation, S-transform,inter band prediction,PSNR.

1. INTRODUCTION

With increase in high data transfer across the network over the past decades, the demand for digital information has increased dramatically. This enormous demand poses difficulties for the current technology to handle storage and transmission resources. The purpose of the image compression is to represent images with less data in order to save storage costs or transmission time and costs. However, the most effective compression is achieved by approximating the original image (rather than reducing it exactly), which is implemented in this paper.

Compression can be achieved in two ways, Predictive coding and Transform coding. In predictive coding the present sample is predicted from previous samples. Delta modulation and Differential pulse code modulation are different techniques in predictive coding. Techniques in Transform coding are Discrete Cosine Transform (DCT), Discrete Fourier Transform (DFT) and Wavelet Transform.

The DCT-based image compression standard is a lossy coding method that will result in some loss of details and unrecoverable distortion. Fourier transform and wavelet transform are some of the common techniques used in compressing an image. Fourier transforms provides only

D.C. Wyld, et al. (Eds): CCSEA 2011, CS & IT 02, pp. 195–207, 2011.
 DOI: 10.5121/csit.2011.1219

frequency information and the temporal information is lost in transformation process, where as wavelets preserves both frequency and temporal information. The wavelet transform is often compared with the Fourier transform, in which signals are represented as a sum of sinusoids.
The main difference is that wavelets are localized in both time and frequency whereas the standard Fourier transform is only localized in frequency. Wavelets often give a better signal representation using Multiresolution analysis, with balanced resolution at any time and frequency.

The use of interband prediction is to improve compression by predicting color channels within an image. Interband prediction is performed instead of an RGB to YUV color space transform as is done in JPEG and JPEG 2000.Interband prediction aids compression when used with wavelet transforms producing gains in PSNR of several dB.

Lossy compression techniques such as JPEG and JPEG 2000 provide the ability to achieve relatively high compression rates at the expense of image quality. These schemes allow the loss to be adjusted so as to trade image quality for bit rate. Both JPEG and JPEG 2000 apply a spectral transform to color images as an initial step before applying a spatial transform. The spectral transform acts to reduce the statistical dependency between different spectral channels. This discussion gives an alternate approach that exploits the statistical dependency to implement interband prediction of the spectral channels.

This paper is organized as follows. Section 1 gives an overview of the image compression techniques used in the industry, comparison between Fourier transform and Wavelet transforms, explaining the advantages of using reversible wavelet transform techniques. Section 2 explains problem formulation of the reversible wavelet transform technique. Step by Step procedure is also explained with required equations. Section 3 deals with compressing a standard color image using MATLAB code explaining salient points. Two standard color images Lenna (512 X 512) and Gold hill (720 X 576) are used to validate this code whose results are documented in this section. Section 4 explains conclusions and future scope pertaining to this paper.

2. PROCESS FORMULATION FOR LOSSLESS COMPRESSION OF COLOR IMAGE

This section explains the process followed in compressing color images using spatial and spectral decorrelation procedures. Steps involved in this process are explained in the following flow chart shown in Figure 1.

2.1 Input

Two experimental test images of different sizes are considered as input images to carry out this process. The color images Lenna of size 512 X 512 and Gold hill of size 720 X 576 are taken.

2.2 Spatial Decorrelation of Color Bands

Traditional color image compression methods typically apply a spectral Decorrelation across the color components first. Then spatial transforms are employed to decorrelate individual spectral bands further. If spectral and spatial transforms are carried out independently, their order is insignificant and can be reversed. This offers the opportunity to apply different spectral transforms to associated color subbands sharing the same scale and orientation. The result is an effective lossless image compression algorithm.

For lossless (or reversible) image compression, it is important to represent transform coefficients with integer numbers. As a result, for progressive-resolution transmission applications, reversible wavelet transforms (RWTs), such as the S-transform or the SP-transform, are often used.

The one-dimensional S-transform reduces the necessary word length by making intelligent use of rounding operations. It successively decimates some input sequence s_k[n] at resolution $r = 2^{-k}$ into truncated average or coarse versions s_{k+1}[n] and associated difference or detail signals d_{k+1}[n] at resolution $r = 2^{-k-1}$. Applying the S-transform to an input signal $s[n] = s_o[n]$ at resolution r = 1, we obtain resolutions that are negative powers of two only, i.e.,$r = 2^{-k}$, $k > 0$.

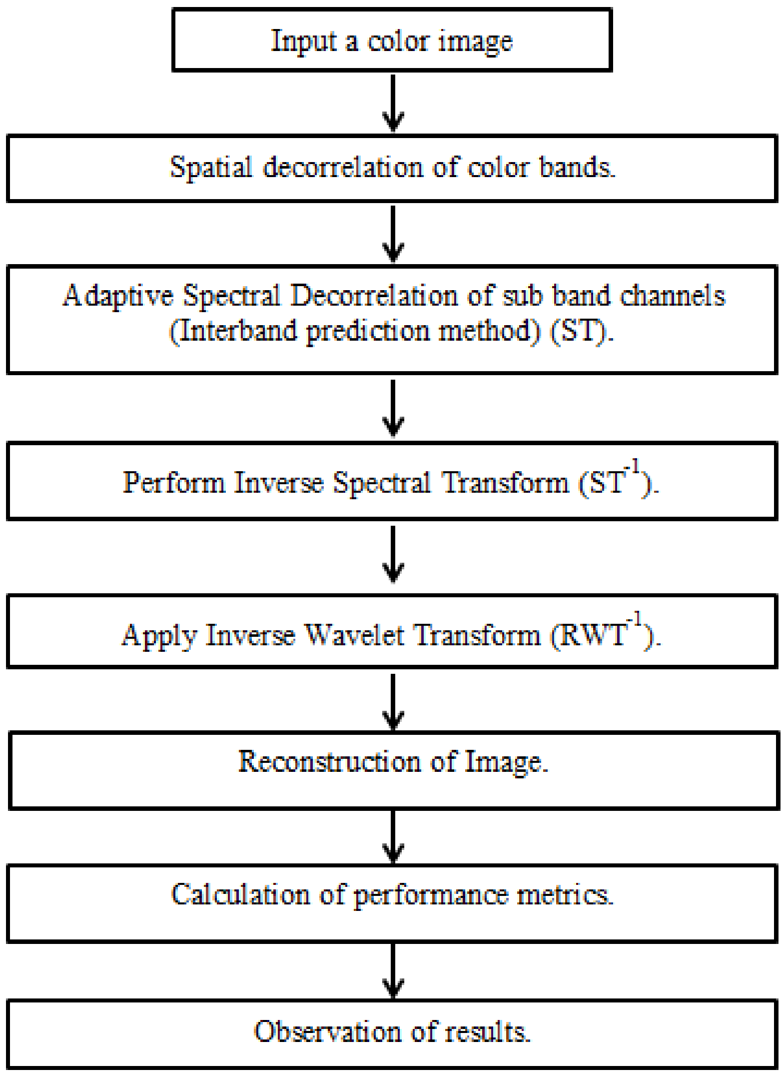

Figure 1. Flow chart for process formulation

Wavelet transform can also be viewed as a pyramid decomposition scheme. A powerful, but conceptually simple structure for representing images at more than one resolution is the image pyramid. An image pyramid is a collection of decreasing resolution images arranged in the shape of a pyramid. The base of the pyramid shows the high resolution representation of the image being processed; the apex contains the low resolution approximation. As we move up the pyramid both the resolution and size decreases.

The detail signals (wavelet coefficients), which are composed of positive and negative integers, on the other hand, require a signed representation. Their number precision, thus, exceeds the original storage format. The significantly lower entropies of difference signals, however, compensate for their longer internal word lengths, since they facilitate the use of efficient coding methods.

A two-dimensional S-transform can be obtained by applying the 1-D S-transform sequentially to the rows and columns of a color image. In this case (truncated) average (or LL) bands at successively lower resolutions are recursively computed by

$$s_{k+1}[m,n,l] = \left\lfloor \frac{\bar{s}_k[2m,l] + \bar{s}_k[2m+1,l]}{2} \right\rfloor \quad (1)$$

Where the (integer) averages along row $\bar{s}_k[r,l]$along row r and incolor channel l are computed via

$$\bar{s}_k[r,l] = \left\lfloor \frac{\bar{s}_k[2m,l] + \bar{s}_k[2m+1,l]}{2} \right\rfloor \quad (2)$$

Wavelet coefficients follow as associated directional differences. In Eq. **(2),** the sample $S_k[m,n,l]$ describes a color pixel at row m**,** column n, and spectral band l ,observed at resolution $r = 2^{-k}$.The red, green and blue color bands are specified by indices l □ {1, 2, 3},respectively. For brevity, the matrix of all pixels in the l^{th} color band at resolution 2^{-k}, $0 \le k \le K$**,** is denoted as

$$s_k[l] = \left\{ s_k[m,n,l] \;\middle|\; 0 \le m < \frac{M}{2^k}, 0 \le n < \frac{N}{2^k} \right\} \quad (3)$$

The parameters M and N are image height and width, respectively. For simplicity, it is assumed that $M = N = 2^K$. This facilitates a K-level wavelet transform.

The rounding operations introduce nonlinearity into the S-transform which produces a noteworthy side-effect. Since both row and column averages are truncated, fractional parts are always discarded. As a result, the transform becomes biased, i.e., integer scaling coefficients at progressively lower resolutions get increasingly smaller than the true local averages. Although this is a minor side-effect of the S-transform, the balanced rounding or BR-transform offers a simple yet effective solution to this problem. It compensates for the round off error by rounding up along image rows while truncating along image columns.

2.3 Spectral Decorrelation of Subband Channels

A reversible wavelet transform is first applied to each color band $s_{k[l]}$ at resolution 2^{-k}. These yields three transform matrices

$$s_k[l] = \left\{ s_k[u,v,l] \;\middle|\; 0 \le u < \frac{M}{2^k}, 0 \le v < \frac{N}{2^k} \right\} (4)$$

Where l □ {1,2,3}. Applying a reversible spectral transform (ST) to $S_{k+l}[l]$, $0 \le l \le 3$, we obtain associated prediction errors denoted as

$$e_{k+1}[l] = \left\{ e_{k+1}[u,v,l] \;\middle|\; 0 \le u < \frac{M}{2^k}, 0 \le v < \frac{N}{2^k} \right\} (5)$$

The combination of inverse spectral transform (ST^{-1}) and inverse reversible wavelet transforms (RWT^{-1}) finally reconstructs the original RGB color channels exactly as explained in Figure 2.

For a particular color l, the transform matrix $S_{k+l}[l]$ can either be considered as an ensemble of transform coefficients or be viewed as a collection of four oriented sub bands. Adopting the second point of view, we describe a color sub band with orientation η at resolution 2^{-k-1}, as

$$S_{k+1}^{(\eta)}[l] = \left\{S_{k+1}^{(\eta)}[u,v,l] \mid 0 \leq u < \frac{M}{2^{k+1}}, 0 \leq v < \frac{N}{2^{k+1}}\right\} \quad (6)$$

for $1 \leq l \leq 3$ and η □ {LL, LH, HL, HH}.

The letters stand for low (L) and high (H) bands corresponding to the separable application of low pass of high pass filters along the rows and columns, respectively. Consequently, the LL-band of S k+1[l] is called$S_{k+1}^{(LL)}[l]$, the LH-band is represented by $S_{k+1}^{(LH)}[l]$, the HL-band referred to as $S_{k+1}^{(HL)}[l]$, and the HH-band finally denoted $S_{k+1}^{(HH)}[l]$.

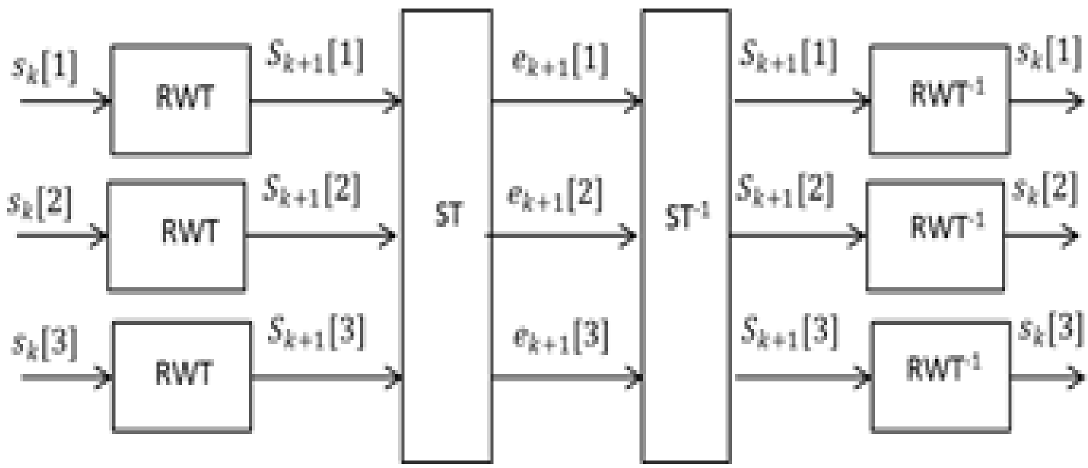

Figure 2.Proposed color decorrelation method

Decomposing of original image into approx. (average) and wavelet (detail) coefficients are shown below for 3 levels RWT.

Performing a K-level wavelet transform on $s_o[l]$, the red band of the input color image with size 2K x 2K, we obtain a total of 3K + 1 oriented red sub bands. They comprise 3K channels with wavelet coefficients and one low pass coefficient representing the mean of the red spectral band. Applying the same RWT to the remaining green and blue color bands, we finally get sets of associated red, green, and blue sub bands which can be effectively spectrally decorrelated. Since there are potentially as many different spectral transforms for a K-level wavelet transform of color images as there are different subbands, it is normally no longer possible to switch the order of the spatial and spectral transforms. Instead, we gain the opportunity to apply an adaptive spectral decorrelation method. It is based on Interband prediction.

2.3.1 Interband Prediction Procedure

The standard JPEG and JPEG 2000 compression schemes convert the image to YUV color space to reduce the statistical dependency between channels. Rather than trying to reduce this correlation between channels by transforming the color space, the proposed scheme tries to utilize this redundancy by working with the R, G and B components of the image.Figure 3.depicts the overall view of Interband Predictor.

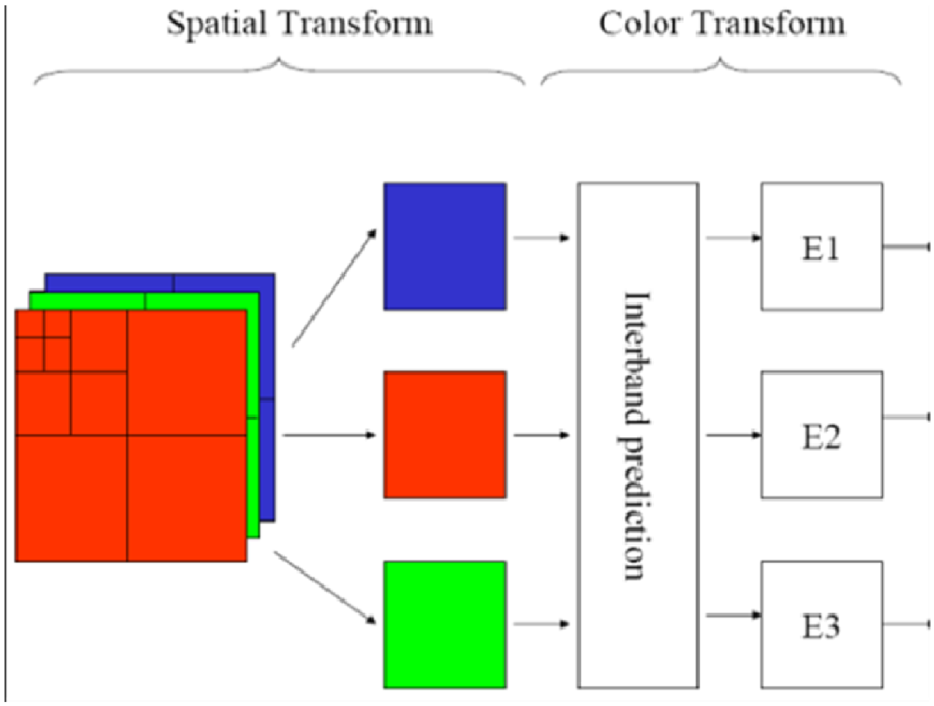

Figure 3. Overall View of Interband Predictor

The steps in in Interband prediction procedure are as follows:

1)Each color channel is independently transformed using a wavelet transform (S) or DCT.

2) Prediction is then performed across the color channels:

(a) Choose an “anchor” color channel A which will not be predicted. This channel will allow the data to be recovered during decompression by serving as the basis for predicting the second channel.

(b) A second color channel B is then predicted from A using a linear predictor.$\hat{B}=\alpha A$(7)

(c) The third color channel is then predicted from A and B using a linear predictor. $\hat{C} = \beta A + C$(8)

Note that the channels A, B and C are chosen so as to minimize the entropy of the residuals after prediction.

3) The prediction errors are given by following formulae.

$e_1=A$ (9)

$e_2 = B - \hat{B}$ (10)

$$e_3 = C - \ddot{C} \quad (11)$$

2.3.2 Interband Prediction Coefficients

For three color bands, at most a two band predictor is needed to predict the third subband from the remaining two. After Interband prediction, each color subband coefficient in the l^{th} band is replaced by its difference with respect to the linear combination of the remaining spectral neighbors. The two band prediction $S_{k+1}^{(\eta)}$ for the l^{th} color subband at resolution 2^{-k-1} and orientation η can be compactly expressed as

$$\hat{S}_{(k+1)}^{(\eta)}[l] = \alpha_1 S_{k+1}^{(\eta)}[i] + \alpha_2 S_{k+1}^{(\eta)}[j] + \bar{S}_{k+1}^{(\eta)}[l] \quad (12)$$

With $i \neq j \neq l$ and $i, j, l \in \{1,2,3\}$

$S_{k+1}^{(\eta)}[i]$ and $S_{k+1}^{(\eta)}[j]$ are the neighboring color subbands, while $\bar{S}_{k+1}^{(\eta)}[l]$ refers to the mean of the lth color subbands. This third order prediction model gives rise to the following procedure for integer subband residuals.

$$e_{k+1}^{(n)}[l] = \left\{ e_{k+1}^{(n)}[u, v, l] \,\middle|\, 0 \leq u < \frac{M}{2^{k+1}}, 0 \leq v < \frac{N}{2^{k+1}} \right\} \quad (13)$$

At spectral location *l*:

1) Compute prediction

$$\hat{S}_{(k+1)}^{(\eta)}[l] = \left[\alpha_1 \left(S_{(k+1)}^{(\eta)}[i] - \left[\bar{S}_{(k+1)}^{(\eta)}[i] \right]_R \right) + \alpha_2 \left(S_{(k+1)}^{(\eta)}[j] - \left[\bar{S}_{(k+1)}^{(\eta)}[j] \right]_R \right) \right]_R + \left[\bar{S}_{(k+1)}^{(\eta)}[l] \right]_R \quad (14)$$

Where $\hat{S}_{(k+1)}^{(\eta)}[l] = E\left(S_{(k+1)}^{(\eta)}[.]\right)$. For high frequency subbands (wavelet coefficients), we have

$$\bar{S}_{(k+1)}^{(\eta)}[i] = \bar{S}_{(k+1)}^{(\eta)}[j] = \bar{S}_{(k+1)}^{(\eta)}[l] = 0 \quad (15)$$

integer values are enforced by using the rounding operator $[.]_R$

2) Compute prediction error.

$$e_{k+1}^{(n)}[l] = S_{(k+1)}^{(\eta)}[l] - \hat{S}_{(k+1)}^{(\eta)}[l] \quad (16)$$

The error subband $e_{k+1}^{(n)}[l]$ comprises differences between actual and predicted color subband coefficients at the spatial locations

3) Encode prediction error and include all necessary side information such as prediction coefficients. Then store or transmit it.

The prediction coefficients α_1 and α_2 are obtained by straight forward application of least square regression formulas**[3]**.

2.3.4 Interband Prediction Order

Reversible linear prediction must be implemented such that it can be resolved based on the information already received. Since loss less prediction involves nonlinear rounding operations, color subband Decorrelation must be carried out sequentially. To this end, an anchor band has to be specified first. Its serves as a reference for predicting the second color subband. Finally the first two subbands provide the basis from which to predict the remaining third. A prediction order must be found such that the overall entropy after color subband prediction is minimized. If we restrict ourselves to single subband prediction, then this problem can be modeled into a graph theoretic problem. While such an approach wholes some promise for multispectral images with hundreds of different bands, better color compression results are obtained when two band predictions is also considered.

Then a scheme for color subband Decorrelation leads to 3! =6 different scenarios. For example, the green subband component can be used as an anchor to predict the red, then red and green can be employed to predict the blue subband coefficients. It determines the prediction order such that approximated sum of subband entropies after prediction is smallest.

It can be shown that an approximation of the first order entropy of a color subband is given by

$$H(X) = \frac{1}{2} log_2(\gamma_x \sigma_x^2) \tag{17}$$

Above equation provides an entropy estimate for color subbands based on their shape factor, γ_x and their varianceσ_x^2.

Two obtain error variances; we select the anchor subband first. Let it be denoted as $S_{k+1}(\eta)$. Subtracting the associated rounded mean $\hat{S}_{(k+1)}^{(\eta)}[i]_R$, we get the first error subband $e_{k+1}(\eta)[i]$.

Next, the anchor band is used to predict the second color subband $S_{k+1}(\eta)[j]$.The resulting prediction error is called $e_{k+1}(\eta)[j]$). Third, $S_{k+1}(\eta)[i]$ and $S_{k+1}(\eta)$ [j] are combined to estimate$S_{k+1}(\eta)$ [l]. This two-step prediction yields the difference band $e_{k+1}(\eta)[l]$. Finally the variances of the error subbands are computed. They are:

$$var\left\{e_{k+1}^{(n)}[i]\right\} = E\left\{\left(S_{(k+1)}^{(\eta)}[i] - \left[\hat{S}_{(k+1)}^{(\eta)}[i]\right]_R\right)^2\right\}$$

$$var\left\{e_{k+1}^{(n)}[j]\right\} = E\left\{\left(S_{(k+1)}^{(\eta)}[j] - \left[\hat{S}_{(k+1)}^{(\eta)}[j]\right]_R\right)^2\right\}$$

$$var\left\{e_{k+1}^{(n)}[l]\right\} = E\left\{\left(S_{(k+1)}^{(\eta)}[l] - \left[\hat{S}_{(k+1)}^{(\eta)}[l]\right]_R\right)^2\right\}$$

Note that *var{$e_{k+1}(\eta)[i]$}* is associated with a zero mean color subband, while *var{$e_{k+1}(\eta)[j]$}*, and *var{$e_{k+1}(\eta)[l]$}* result from prediction residuals.

Once the variances have been computed, entropies of their associated subbands are estimated. The sum of entropies of all three transform subbands at resolution 2-k-1 and orientation n is called $H_{k+1}(\eta)$. According to equation (5) it can be approximated by

$$H_{k+1}^{(\eta)} = \frac{1}{2}\left(log_2(\gamma_i\gamma_j\gamma_l) + log_2\left(var\left\{e_{k+1}^{(n)}[i]\right\} var\left\{e_{k+1}^{(n)}[j]\right\} var\left\{e_{k+1}^{(n)}[l]\right\}\right)\right)$$

The shape factors γ_i, γ_j, γ_l are associated with pdf's of $e_{k+1}^{(n)}[i], e_{k+1}^{(n)}[j]$ and $e_{k+1}^{(n)}[l]$ respectively.

Each prediction yields a different value for $H_{k+1}^{(\eta)}$. The best ordering is found by selecting the prediction sequence resulting in a smallest value for $H_{k+1}^{(\eta)}$for simplicity, we assume that the product of shape factors remains constant regardless of the prediction sequence chosen. The underlying assumption is that the overall statistical character of the prediction errors remains the same regardless of the prediction order. Since the logarithm is monotonically increasing, we only need to compare products of error variances.

2.4 Calculations of Performance Metrics

2.4.1 Entropy

In information theory, entropy is a measure of the uncertainty associated with a random variable. In this context, the term usually refers to the Shannon entropy, which quantifies the expected value of the information contained in a message, usually in units such as bits. Entropy is a measure of disorder, or more precisely unpredictability. For example, a series of coin tosses with a fair coin has maximum entropy, since there is no way to predict what will come next. A string of coin tosses with a two-headed coin has zero entropy, since the coin will always come up heads. If a compression scheme is lossless, that is, we can always recover the entire original message by uncompressing, then a compressed message has the same total entropy as the original, but in fewer bits. That is, it has more entropy per bit. This means a compressed message is more unpredictable, which is why messages are often compressed before being encrypted. Entropy effectively bounds the performance of the strongest lossless (or nearly lossless) compression possible.

It is defined as average information per source output denoted asH(z).This is also known as uncertainty.

$$H(X) = \frac{1}{2} \log_2(\gamma_x \sigma_x^2)$$

provides an entropy estimate for color subbands based on their shape factor, γ_x, and their variance σ_x^2.

2.4.2 PSNR (Peak Signal to Noise Ratio)

The PSNR is most commonly used as a measure of quality of reconstruction of image compression. The signal in this case is the original data, and the noise is the error introduced by compression.

$$\text{PSNR} = 20 * \log_{10}\left(\frac{255}{\sqrt{\text{mean of square of the err.signal}}}\right)$$

Where,Err signal=input image -- output image

2.4.3 Average Bit Rate Per Pixel (bpp)

It is based on compressed file size and takes all the side information necessary to losslessly reconstruct the original image. The lesser the value of bpp the better the compression.

Average bit rate per pixel (bpp) R = (total file length (in bits)) / no. pixels.

2.4.4 Compression Ratio (C_R)

The compression ratio is equal to the size of the compressed image to the size of the original image. This ratio gives an indication of how much compression is achieved for a particular image. Most algorithms have a typical range of compression ratios that they can achieve over a variety of images. Because of this, it is usually more useful to look at an average compression ratio for a particular method.

$$C_R = \left(\frac{\text{No. of bits in input image} - \text{No. of bits in compressed image}}{\text{No. of bits in input image}}\right)$$

3. RESULTS

Two standard color images Lenna (512 X 512) and Gold hill (720 X 576) are used to validate this code whose results are discussedhere.

Table1: Results summary of Lenna and Goldhill images using RWT

Images	Lenna	Goldhill
No. of rows (M):	512	576
No. of columns (N):	512	720
No. of color bands (L)	3	3
No. of compression levels (K):	4	4
Peak Signal to Noise Ratio (PSNR):	36.88	35.66
Total number of bits in i/p image:	6291456	9953280
Total number of bits in compressed image:	1141500	1786100
Percentage of compression:	81.86%	82.06%
average bit rate per pixel(bpp):	4.35	4.31

Table1 gives an insight to salient results like PSNR, C_R and bpp. Results indicate higher compression ratios and lower bpp. The higher the PSNR indicate good quality of reconstruction of an image.

Table 2: bpp comparison chart

Images	$R_{ST}^{(S)}$	$R_{ST}^{(TT)}$	$R_{col}^{(CREW)}$
Lenna	4.35	11.115	11.113
Gold hill	4.31	12.540	12.554

Table 2 gives the comparison based on the average bit rate per pixel (bpp) simply denoted by R. The bit rates obtained with S transforms followed by spectral decorrelation is indicated $R_{ST}^{(S)}$. The outcomes associated with TT filter band are labeled $R_{ST}^{(TT)}$ and compression with reversible embedded wavelet is labeled with $R_{col}^{(CREW)}$. The results of last two columns referred in table 2 are taken from **[1].** One can observe the lowest bit rates with the implemented method.

4. Conclusions and Future Scope

In this paper we have demonstrated that interband prediction between RGB color channels can be used to improve compression when used with wavelet transforms. The results of testing revealed improved gains of several Db. Faster and exact reconstruction of image with minimum entropy and variance is observed. This technique optimizes progressive image transmission with better compression ratios and high PSNR values. S-Transform with predictor completely eliminates the contouring artifacts usually present in bit plane coded images. The implemented algorithm can achieve bit rates that are 20% less than results obtained with comparable lossless image compression techniques supporting progressive resolution transmission of color images.

Interband prediction does not perform well if the image contains relatively low correlation between the color channels. In this case the predictor is unable to accurately predict the color channels and thus the error signals have a high variance, resulting in large entropy. A little improvement beyond spatial decorrelation should be expected. A good reversible sub band transforms are essential in this case. They are normally well designed filter banks characterized by longer analysis high pass filters with higher stop band attenuation.

Fortunately, in many cases color bands are strongly correlated. Then a lossless image compression for progressive resolution transmission requires a simple S-transform followed by adaptive spectral prediction.

Acknowledgements

The authors would like to acknowledge the infrastructural support provided by VGST DST Gov. of Karnataka to establish the center of excellence in Image and audio processing and implement the above project. The authors would like to thank the Management and Principal CMRIT for all the support.

References

[1] **N. Strobel, S. K. Mitra, and B. S. Manjunath.***Reversible wavelet and spectral transforms for lossless compression of color images*. In Proc. IEEE Intern. Conf. Image Processing, ICIP-98, volume3, pages 896–900, Chicago, IL, Oct 1998.

[2] **Glen Gibb.** *Wavelet coding of color images using a spectral transform in the sub band domain***.** Stanford, 2006.

[3] **Fox, John.***"Linear Least Squares Regression." In Applied Regression Analysis, Linear Models, and Related Methods,*85-111. Thousand Oaks, CA: Sage, 1997.

[4] **Grewal, B.S.** *Higher Engineering Mathematics*, Khanna Publishers, New Delhi, 2010.

[5] **Woods and Gonzalez.** *Digital Image Processing Using Matlab*, Prentice Hall, 2004.

[6] **Soman, K. P. and Ramchandran, K. I.** *Insight into Wavelets from Theory to Practice***.** Prentice-Hall of India, 2010.

[7] **S.R Tate,** *Band ordering in lossless compression by multi spectral images.* IEEE Transactions on Computers, Volume 46 Issue 4, April 1997.

[8] **Stephen J. Chapman,** *MATLAB Programming for Engineers, 4e,* Cengage Learning, 2008.

[9] **Sanjit K. Mitra,** *Digital Signal Processing: A Computer-Based Approach, 4e,* McGraw- Hill, 2010.

[10] **N. Strobel, S. K. Mitra, and B. S. Manjunath.** "Lossless compression of color images for digital image libraries,"*In Proceedings of the 13th Inter-national Conference on Digital Signal Processing, volume* 1, pages 435-438, Santorin, Greece, 1997..

[11] **W.K.Pratt, "**Spatial transform coding of color images,"*IEEE Transactions on Communications Technology,* 19(6):980-992, 1971.

[12] **O.Rioul,** "A discrete-time Multiresolution theory," *IEEE Transactions on Signal Processing,* 41(8):2591-2606, 1995.

[13] **M.J.Gormish, E.Schwartz, A.Keith, M.Boliek and A.zandi,** "Lossless and nearly lossless compression for high quality images" *in Proceedings of the SPIE*, volume 3025, SanJose, CA, February 1997.

[14] **Olivier Rioul and Martin Vetterli,** "Wavelets and Signal Processing", *IEEE Trans. on Signal Processing,* Vol. 8, Issue 4, pp. 14 - 38 October 1991.

[15] **Boliek, M., Gormish, M. J., Schwartz, E. L., and Keith**, "A. Next Generation Image Compression and Manipulation Using CREW", *Proc. IEEE* ICIP, 1997.

[16] **A. Zandi, J. Allen, E. Schwartz, and M. Boliek**, "CREW: Compression with reversible embedded wavelets," *IEEE Data Compression Conference*, Snowbird, UT, pp. 212–221, March 1995.

[17] **A. Said and W. A. Peralman**, "An Image Multiresolution Representation for Lossless and Lossy Compression," *IEEE Trans. on Image Processing*, Vol. 5, pp. 1303-1310, September 1996.

[18] **Amir Said, and Pearlman**. **W. A**, " A New, Fast, and Efficient Image Codec Based on Set Partitioning in Hierarchical Trees" *IEEE Trans. Circuit and systems for Video Technology*, vol. 6, no. 3, pp. 243-250, June 1996.

[19] **Asad Islam & Pearlman**, "An embedded and efficient low-complexity, hierarchical image coder", Visual Communication and Image processing" *99 proceedings of SPIE.,*Vol 3653,pp294-305, Jan., 1999.

[20] **J. Shapiro**," Embedded image coding using zero tress of wavelet coefficients," *IEEE Trans. Signal Processing* **41**, pp. 3445-3462, Dec. 1993.

Authors

B.E, Electronics and Communication and M Tech, Industrial Electronics from Vishveshvaraya technological University and pursuing Ph.D. in Dr M G R Educational and Research Institute, Chennai; Having more than 20 years of experience in Industry and Educational Institutions handling various responsibilities and currently working in CMR Institute of Technology, Bangalore as professor and head, department of electronics ; established several labs &conducted 2 National Conferences with the support from DST/DIT/ISRO/DRDO/ISTE and conducted several courses & FDP; Published 16 papers in national/International conferences and Journals.

The area of interest is VLSI and Embedded Systems; ISTE Life member.P.G. Scholar in Digital Electronics from CMR Institute of Technology.Department of Electronics and communication Bangalore, the area of interest is Analog and Digital Electronics, Image processing and power Electronics.